Multimodal residual stress evaluation following one-sided dimpling in a Ti-6Al-4V alloy plate

Igor A. Zorin*
HSM lab, Center for Engineering Systems and Sciences, Skoltech, Moscow, Russia
igor.zorin@skoltech.ru, http://orcid.org/0000-0001-9349-2494

Vladimir S. Pisarev, Svyatoslav I. Eleonsky
The Zhukovsky Central Aero-Hydrodynamical Institute (TsAGI), Moscow, Russia
VSP5335@mail.ru, http://orcid.org/0000-0002-5378-609X
juzzepka@mail.ru, http://orcid.org/0000-0003-4345-067X

Aleksandr S. Elkin
Center for Material Technologies, Skoltech, Moscow, Russia
CASM&T, Moscow Aviation Institute, Moscow, Russia
aleksandr.elkin@skoltech.ru, http://orcid.org/0000-0003-2157-3425

Galina V. Tyurina
Laboratory of Accelerated Particles "LUCh", NUST MISIS, Moscow, Russia
tiurina.gv@misis.ru, http://orcid.org/0009-0004-1314-7826

Eugene S. Statnik, Alexey I. Salimon, Alexander M. Korsunsky
HSM lab, Center for Engineering Systems and Sciences, Skoltech, Moscow, Russia
CASM&T, Moscow Aviation Institute, Moscow, Russia
Laboratory of Accelerated Particles "LUCh", NUST MISIS, Moscow, Russia
eugene.statnik@skoltech.ru, http://orcid.org/0000-0002-1105-9206
a.salimon@skoltech.ru, http://orcid.org/0000-0002-9048-8083
a.korsunsky@skoltech.ru, http://orcid.org/0000-0002-3558-5198

ABSTRACT. Residual stress significantly influences the mechanical performance, fatigue resistance, and structural reliability of titanium alloys used in engineering applications. This study investigates the residual stress distribution induced by one-sided dimpling in Ti-6Al-4V alloy using a combined experimental–numerical approach. Localized plastic deformation produced by spherical indentation generates stress fields that are difficult to characterize with a single technique. Residual stresses in the plane were evaluated using Focused Ion Beam–Digital Image Correlation (FIB-DIC) and Electronic Speckle Pattern Interferometry (ESPI). To evaluate the residual stress through the sample thickness, the cross-section warp method was used,

Citation: Zorin, I., Pisaerv, V., Eeonsky, S., Elkin, A., Tyurina, G., Statnik, E., Slimon, A., Korsunsky, A., Multimodal residual stress evaluation following one-sided dimpling in a Ti-6Al-4V alloy plate, Fracture and Structural Integrity, 77 (2026) 1-12.

Received: 13.2.2026
Accepted: 23.03.2026
Published: 03.04.2026
Issue: 07.2026

that analyze the warping (deplanation) of the cross-section after cutting and provides an alternative way to infer the internal stress distributions and complements existing measurement techniques. The results reveal compressive residual stresses near the dimpled surface and tensile stresses developing at greater depths due to elastic recovery and equilibrium constraints. Finite element simulations match the experimentally observed stress distributions and confirm the reliability of the proposed methodology. The validated finite element model provides a predictive framework for future studies, enabling systematic analysis of how indentation depth and the indenter diameter affect the magnitude and distribution of compressive residual stresses, and supporting the optimization of dimpling parameters for improved structural performance.

KEYWORDS. Residual stress, Cross-section warp method, Focused Ion Beam - Digital Image Correlation (FIB-DIC), Electronic Speckle Pattern Interferometry (ESPI), Finite Element Modeling (FEM).

INTRODUCTION

Residual stress plays a critical role in determining the mechanical performance, fatigue resistance, and structural integrity of engineering components [5,14,17]. This stress arises as a consequence of non-uniform plastic deformation, thermal gradients, or phase transformations during manufacturing and service processes [21,22]. In many high-performance structural materials, particularly titanium alloys used in aerospace and energy applications, residual stresses can significantly influence crack initiation, crack propagation, and long-term durability [5,11,19]. Consequently, reliable experimental and computational methods for their determination remain an important topic of research in materials science and structural mechanics [4,16]. Residual stress fields generated by local plastic deformation processes are typically heterogeneous and three-dimensional. Their distribution depends on the geometry of the component, the loading path during manufacturing, and the mechanical response of the material. One example of such a process is one-sided dimpling (indentation), which is widely used in manufacturing and structural modification technologies. The process involves pressing a spherical indenter into the surface of a component, inducing localized plastic deformation and generating a characteristic distribution of compressive and tensile residual stresses. Despite the relative simplicity of the process, the resulting stress field is complex due to the interaction between plastic deformation near the surface and elastic constraints in the surrounding material.

From a qualitative perspective, the general scheme of residual stress distribution through the thickness after one-sided dimpling is well understood. Typically, compressive stresses develop in the near-surface region beneath the indentation, while tensile stresses appear deeper within the material and squeeze up to boundaries as a result of elastic recovery and force equilibrium. Such stress states are of particular interest because surface compressive stresses are known to improve fatigue performance and resistance to crack initiation. However, the complete three-dimensional stress distribution inside the body remains difficult to quantify experimentally. Fig. 1 schematically illustrates the expected distribution of residual stresses through the thickness after one-sided dimpling.

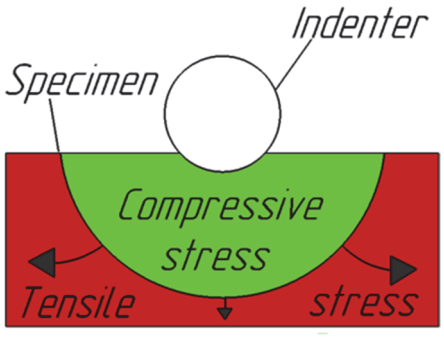

Figure 1: Scheme of residual stress distribution through thickness after one-sided dimpling.

Although many experimental techniques have been developed to evaluate residual stresses, most of them are primarily sensitive to surface or near-surface stress states. Methods such as X-ray diffraction, hole-drilling, or optical interferometric techniques are widely used for the measurement of in-plane stresses at the surface of components [6,9]. These approaches provide valuable information about residual stresses that directly affect surface damage and fatigue initiation. Nevertheless, the distribution of stresses through the thickness of a deformed body often remains insufficiently characterized. In many practical situations, particularly in components subjected to localized plastic deformation, the stress gradient along the depth direction can be substantial. Therefore, surface measurements alone are insufficient to reconstruct the full three-dimensional stress state.

This limitation has motivated the development of integrated experimental–computational approaches capable of combining information obtained from different spatial scales. In particular, the use of complementary experimental techniques allows one to capture both global and local features of the field of residual stress. At the same time, validated numerical models can be employed to reconstruct stress distribution in the entire volume of the body. Such hybrid strategies significantly improve the reliability of residual stress evaluation compared with the use of any single method.

The present study proposes a comprehensive methodology for determining residual stresses both on the surface and within the volume of a heterogeneous deformed body produced by one-sided dimpling. The approach integrates several experimental techniques with finite-element modeling in order to obtain a consistent and experimentally validated description of the residual stress field. The principal idea is to combine measurements performed at different length scales and then use them to validate and refine the numerical model describing the deformation process.

The first component of the proposed methodology focuses on accurate experimental characterization of the in-plane residual stresses at the surface. For this purpose, two complementary techniques are employed: Electronic Speckle Pattern Interferometry (ESPI) and Focused Ion Beam – Digital Image Correlation (FIB-DIC). These methods operate at different spatial scales and provide independent measurements of stress-induced displacement fields. ESPI enables full-field optical measurements of surface displacements associated with stress unloading during hole drilling, offering high sensitivity and the ability to analyze relatively large areas around the indentation. In contrast, the FIB-DIC method provides high-resolution measurements at the micro-scale by combining controlled material removal using a focused ion beam with digital image correlation in a scanning electron microscope. The combined use of these techniques enables reliable characterization of residual stress.

The second key component of the proposed methodology addresses the more challenging problem of determining residual stresses within the volume of the body. In many previous studies devoted to indentation-induced residual stresses, the analysis has been restricted mainly to the surface or near-surface regions. However, the internal stress distribution through the thickness plays an equally important role in structural performance and may significantly affect the mechanical response of the component under service loading. To address this issue, the present work introduces an original technique based on the joint use of profilometric measurements of the cross-section of a divided specimen and finite-element analysis – the cross-section warp method.

The principle of this method is based on stress unloading induced by separating the deformed body into two parts. When a specimen containing residual stresses is cut, the release of internal constraints leads to elastic deformation of the newly formed surfaces. The resulting displacement field reflects the original stress distribution inside the material. By measuring the surface profile of the cross-section using optical profilometry, it becomes possible to obtain quantitative information about the deformation caused by stress relief. In the present work, these experimental measurements are directly compared with the results of finite-element simulations of the cutting process. Such a direct comparison allows validation of the calculated residual stress distribution through the thickness without solving a reverse reconstruction problem known as contour method [15].

The integration of these experimental and computational tools forms a unified framework for residual stress evaluation. Surface stresses measured by ESPI and FIB-DIC are first used to validate the finite-element model of the dimpling process. Once validated, the model provides a physically consistent description of the three-dimensional stress field generated by indentation. The subsequent simulation of specimen cutting allows prediction of the deformation of the cross-section after stress relief, which can then be compared with profilometric measurements. This multi-stage validation strategy significantly increases confidence in the reconstructed residual stress field.

The main advantage of the methodology lies in its complementary nature. Instead of relying on a single measurement technique, the approach combines macro-scale optical interferometry, micro-scale ion-beam-based stress relaxation measurements, and numerical modeling supported by experimental validation. This integration enables the reliable determination of both surface and volumetric residual stresses in complex deformed bodies. Furthermore, the method potentially can be applied to a wide range of materials and manufacturing processes where localized plastic deformation generates heterogeneous residual stress fields.

The objective of the present study is thus to develop and show a comprehensive experimental–computational approach for residual stress determination in both the surface layer and the bulk of a deformed body. The methodology integrates ESPI and FIB-DIC techniques for surface stress evaluation with an original cross-section profilometry–FEM strategy for validating the stress distribution through the thickness. By combining these methods within a unified framework, the study aims to provide a robust and experimentally supported analysis of residual stress formation after one-sided dimpling.

MATERIALS AND METHODS

A plate of dimensions 30×30×12 mm made from titanium alloy Ti-6Al-4V (Russian variant VT6) was deformed using a 16 mm diameter hardened steel spherical indenter under the applied load of 13 kN to a dimpling depth equal to 1 mm (Fig. 2a, b). The titanium plate was investigated in the as-received condition (high temperature rolling and normalization), since this condition corresponds to the typical state in which the material is supplied for industrial processing. The study focused on the residual stress redistribution caused by the dimpling process while the initial residual stress field of the plate was deliberately neglected.

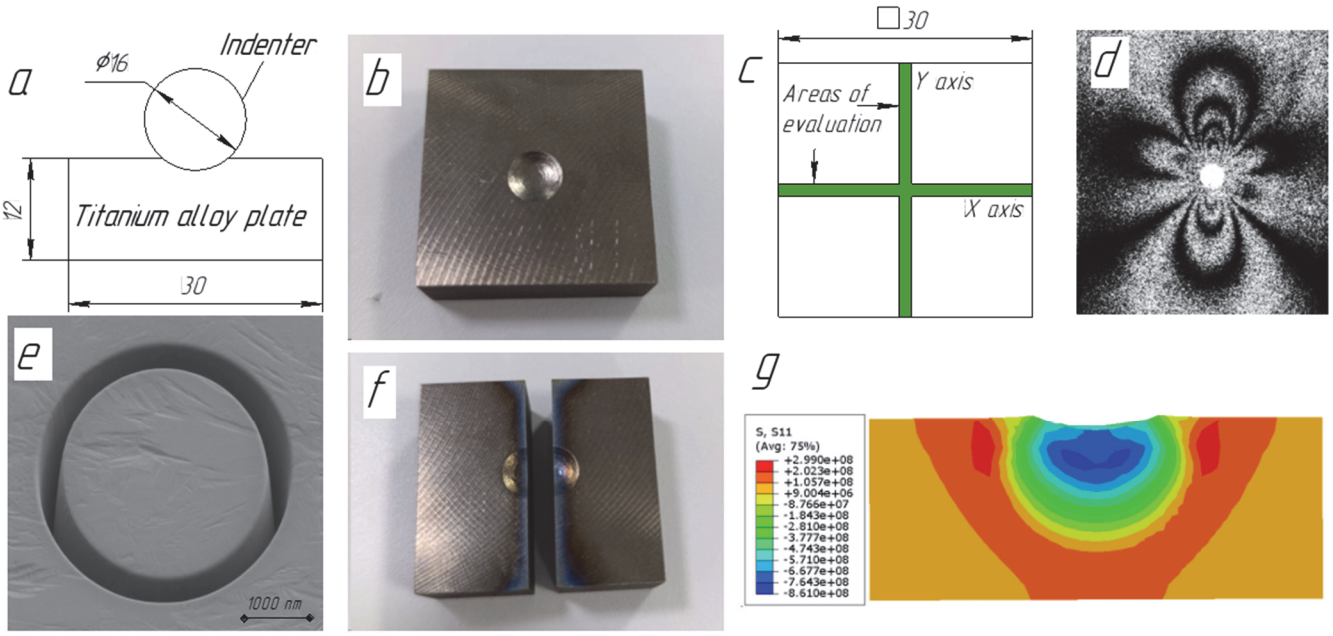

Figure 2: Materials and methods used for investigation: a) Sketch of one-sided dimpling; b) Plate after dimpling; c) Scheme of residual stress in-plane evaluation; d) ESPI interferogram; e) FIB-DIC ring; f) Specimen after cutting; g) FEM model.

Electronic Speckle Pattern Interferometry (ESPI)

ESPI was employed to obtain full-field measurements of in-plane displacement induced by local stress unloading during blind-hole drilling [7,13]. The use of ESPI in the present study is motivated by the need for non-contact, high-sensitivity characterization of residual stresses over a relatively large surface area surrounding the dimple, providing reliable experimental data for validation of the finite element model. The final residual stress was determined across the X and Y plane on the surface of the specimen (Fig. 2c) and then recalculated into cylindrical coordinates.

ESPI is based on laser interferometry and records changes in the speckle pattern formed by coherent illumination of a rough surface (Fig. 3). Two digital images of the area investigated are acquired in the initial and stress-relieved states. Subtraction of these images produces interference fringe patterns (Fig. 2d) that represent contours of equal displacement. In the hole-drilling method, drilling introduces a local stress unloading, and the resulting fringe pattern reflects the corresponding deformation field. It should be noted that the interferogram shown in Fig. 2d is not expected to be perfectly symmetrical. In ESPI measurements, the recorded fringe pattern corresponds to the projection of the displacement field onto the optical sensitivity direction defined by the illumination geometry. In addition, stress unloading produced by one-sided dimpling and blind-hole drilling is not strictly axisymmetric because of local plastic deformation and finite specimen geometry. Therefore, a certain asymmetry of the interference fringes can appear and reflect the actual displacement-relief field rather than a measurement artifact.

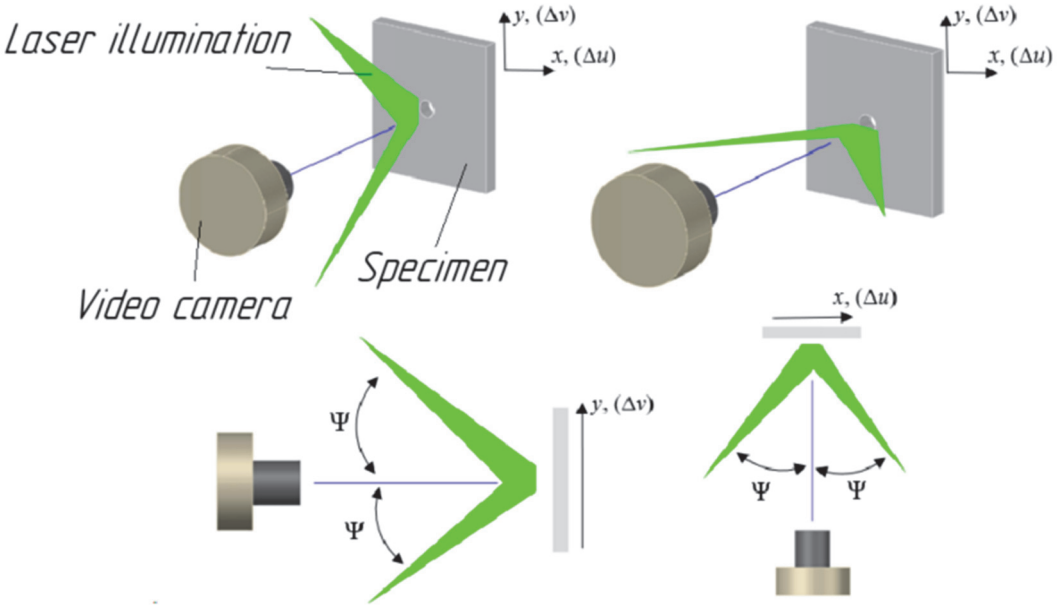

Figure 3: Schematic diagram of interference fringe patterns capturing (ESPI method).

The in-plane displacement components along two orthogonal directions are measured using symmetrical dual-beam illumination and normal observation, allowing determination of hole diameter increments required for residual stress calculation. Residual stress can be evaluated using Eqns. 1, 2:

$$\sigma_r = \frac{E}{2r_0}\left\{\frac{a\Delta u + b\Delta v}{a^2 - b^2}\right\} \quad (1)$$

$$\sigma_\theta = \frac{E}{2r_0}\left\{\frac{a\Delta v + b\Delta u}{a^2 - b^2}\right\} \quad (2)$$

where E- elastic modulus; r_0- diameter of the probing hole; Δu and Δv tangential displacement components characterizing the increments of hole diameters; a = (α_1^m - 1), b = (α_2^m - μ). Kirsch's theoretical solution, which gives values of α_1^m= 3 and α_2^m= 1, ensures reliable obtaining of residual stress values.

The technique provides several advantages, including contactless measurement, high displacement sensitivity (sub-micrometer level), rapid data acquisition, and automated digital processing over a field of view sufficient to capture the deformation zone. In this work, ESPI provides reliable macroscopic in-plane stress evaluation that complements the localized FIB-DIC measurements.

Focused Ion Beam – Digital Image Correlation (FIB-DIC)

The FIB-DIC method is based on the principle of controlled material removal and measurement of the associated elastic strain relief [10]. A focused ion beam is used to mill a predefined micro-scale geometry (in this work, a ring-core) into the surface. The dimensions of the micro ring-core must be carefully selected relative to the material's microstructural features, particularly the average grain size, as this directly influences the scale and interpretation of residual stress evaluation using the FIB-DIC approach. To address this point rigorously, prior to ring-core milling we perform comprehensive microstructural characterization using electron backscatter diffraction (EBSD) and Energy-dispersive X-ray spectroscopy (EDS). The creation of new traction-free surfaces causes redistribution and partial relaxation of the pre-existing residual stresses. The resulting surface displacement field is recorded using high-resolution scanning electron microscope (SEM) imaging and quantified by digital image correlation (Fig. 2e). By tracking the motion of surface features with sub-pixel accuracy, full-field displacement and strain maps are obtained. Residual stress is then determined from the measured strain relief using elastic solutions across the X and Y plane on the surface of the specimen (Fig. 2c) and recalculated into cylindrical coordinates.

Also, it should be noticed that FIB-DIC measurements in the dimpled area were carried out on a small local area of the indentation surface. Since the ring-core diameter comparable to a few micron scales is much smaller than the characteristic radius of curvature of the indentation, the analyzed surface region can be considered locally planar. Therefore, distortions associated with the surface curvature have a negligible influence on the displacement measurements. Additionally, the sample was oriented in the SEM so that the analyzed area was close to the normal viewing direction, minimizing possible projection errors in the DIC analysis.

The strain relief at every step can be calculated using Eqn. 3:

$$(f(\Delta\varepsilon_\infty, z) = 1.12\Delta\varepsilon_\infty \times \frac{z}{1+z}[1+\frac{2}{(1+z^2)}]) \quad (3)$$

where z=h/0.42d is the milled depth, d is the core diameter, and $\Delta\varepsilon_\infty$ is the full strain relief at an infinite milling (or full) depth.

The technique offers several important advantages. First, it provides sub-micron lateral resolution and depth resolution on the order of a few hundred nanometers, enabling the analysis of highly localized stress fields and near-surface gradients. Second, the method is largely material-independent and applicable to both crystalline and amorphous materials, unlike diffraction-based techniques that require crystallinity. Third, the use of low ion currents allows minimally invasive material removal, making FIB-DIC a semi-destructive method with limited disturbance to the surrounding stress field. In addition, the ring-core geometry produces efficient and nearly uniform strain relief in the central island, improving the accuracy and robustness of stress evaluation.

In the context of the present work, FIB-DIC complements ESPI-based hole drilling by providing local verification of the in-plane stress components in the vicinity of the dimple, where strong stress gradients are expected. The combined use of macro- and micro-scale relaxation techniques ensures reliable characterization of the residual stress field and supports high-fidelity validation of the finite element model.

The cross-section warp method

The cross-section warp method is an approach that uses the cross-section warp following electric discharge cutting (deplanation) as the target for numerical model matching and refinement. The method is based on the principle of stress relaxation caused by material separation and the subsequent measurement of the deformation induced by the release of internal stresses.

In this procedure, the specimen was first rigidly clamped in a fixture to preserve its original deformation state. A through-thickness cut was then introduced using wire electrical discharge machine (WEDM) (Fig. 2f), which provides precise material separation with minimal mechanical loading [1,12]. The cut creates new traction-free surfaces, causing redistribution and partial relaxation of the residual stresses (Fig. 4a, b). As a result, the separated halves undergo elastic deformation, leading to out-of-plane displacement (warp) of the newly formed cross-sectional surfaces.

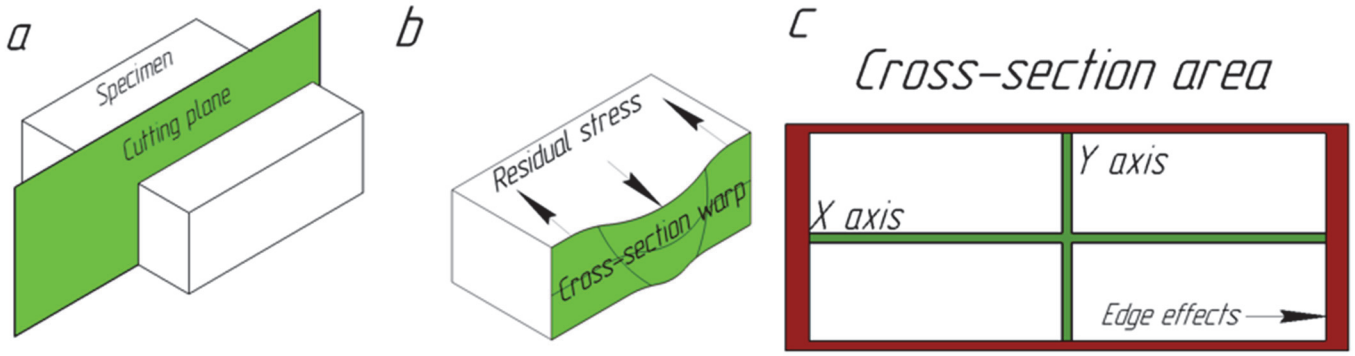

Figure 4: Schematic diagram of the cross-section warp method: a) Cutting the specimen using an electric discharging machine; b) Displacement distribution after cutting; c) Scheme of displacement evaluation lines including experimental edge effects.

During WEDM cutting, material removal occurs through a sequence of localized electrical discharges, which may produce a thin recast layer on the cut surface. However, the associated thermal effects are confined to a very shallow region near the surface (typically a dozen micrometers) and do not significantly affect the reconstructed residual stress field when appropriate machining parameters are used. The surface appearance in Fig. 2f corresponds to this typical WEDM recast

layer rather than to a bulk thermal gradient in the specimen. To ensure reliable measurements, the analysis was restricted to the central region of the cross-section 8×20 mm (Fig. 4c), excluding boundary areas affected by thermal and edge effects associated with the WEDM process.
After cutting, the surface topography of the exposed cross-section was measured using optical profilometry. The obtained displacement field represents the cumulative deformation associated with the release of the original residual stresses across the specimen thickness. The experimentally measured displacement profiles were then compared with the corresponding deformation predicted by the finite element simulation of the cutting step. This direct comparison provides an independent validation of the computed through-thickness residual stress field without solving an inverse reconstruction problem.

Finite Element Modeling (FEM)

Finite element analysis was performed using Abaqus 2023 to simulate the complete mechanical history of the process, including dimpling, unloading, and subsequent stress relaxation after cutting (Fig. 2g). The model represents a 30 × 30 × 12 mm Ti-6Al-4V plate defined as a three-dimensional deformable solid with elastic–plastic material behavior. The material properties included a Young's modulus of 115 GPa, Poisson's ratio of 0.32, density of 4550 kg/m³, yield strength of 950 MPa, ultimate compressive strength of 1100 MPa, and compressive strain of 32%. The material parameters were taken from the ASM Handbook [2] for the titanium alloy and were used to define the plastic deformation behavior in the numerical model. An isotropic hardening plasticity model with a linear hardening approximation of the stress–strain curve was adopted to describe the material response under large local deformation during indentation.
The plate was discretized using 8-node linear brick elements with reduced integration (C3D8R) and a characteristic element size of 0.1 mm in the dimpled area and 0.5 mm in the remaining part of the model. The spherical indenter (Ø16 mm) was modeled as a discrete rigid body using 4-node rigid surface elements (R3D4), with a mesh size of 0.5 mm. Surface-to-surface contact with finite sliding was defined between the indenter and the plate, with the deformation process controlled by prescribed indenter displacement to reproduce the required dimpling depth, followed by complete unloading to capture the residual stress state. Boundary conditions were applied to prevent rigid body motion while minimizing artificial constraint of the deformation field. In the finite element model, rigid-body motion was prevented by applying a ZSYMM boundary condition on the bottom surface of the specimen (U3=UR1=UR2=0). In addition, the lateral faces of the modeled cube were constrained by setting U1=U2=0. Contact between the indenter and the titanium plate was defined using a Coulomb friction law with a friction coefficient of $\mu = 0.3$. These constraints were introduced only to stabilize the numerical solution and do not influence the local stress–strain evolution in the dimpling region. After validation of the in-plane residual stresses, the cutting was simulated to reproduce the cross-section warp experiment. Material removal along the cutting plane was modeled by drastically reducing the Young's modulus of the affected elements from 115 GPa to 115 kPa, thereby creating a virtually traction-free boundary and allowing elastic stress relaxation. This operation effectively removes the stiffness of the elements in the cut region using a predefined field function and reproduces the mechanical separation of the material. The separation stage was implemented after the stress unloading step, and no external loads were applied during this stage; the model was allowed to reach a new equilibrium state corresponding to the redistribution of the residual stress.
The resulting displacement field was extracted and directly compared with profilometry measurements to validate the through-thickness residual stress distribution. All these techniques provide an experimental-computational approach to one-sided dimpling technology.

RESULTS AND DISCUSSION

The initial part of research started with microstructure investigation of titanium alloy plate using EBSD and EDS techniques. This step is mandatory for FIB-DIC method, the microstructure evaluation is necessary because of the size and place of micro-ring core. These factors have a great influence on scale and interpretation of residual stress value. Fig. 5a shows the grain orientation map of the plate, the percentage of large-angle boundaries is equal to 100% and average grain size is about 50 μm (Fig. 5b). It is also observed that BCC phase and texture are absent.
The further research of residual stress evolution in the Ti-6Al-4V (Russian standard VT-6) specimens was structured according to a three-stage material deformation model: (i) localized plastic deformation induced by one-sided dimpling, (ii) subsequent unloading, and (iii) stress redistribution following specimen cutting (for in-depth stress mapping). The FEM model was developed to sequentially replicate all three stages, thereby capturing the full history-dependent stress state. Model validation was performed in two steps. The first step focused on the in-plane residual stress field after unloading. To ensure accurate validation, two independent experimental techniques were employed: FIB-DIC and hole drilling combined with ESPI.

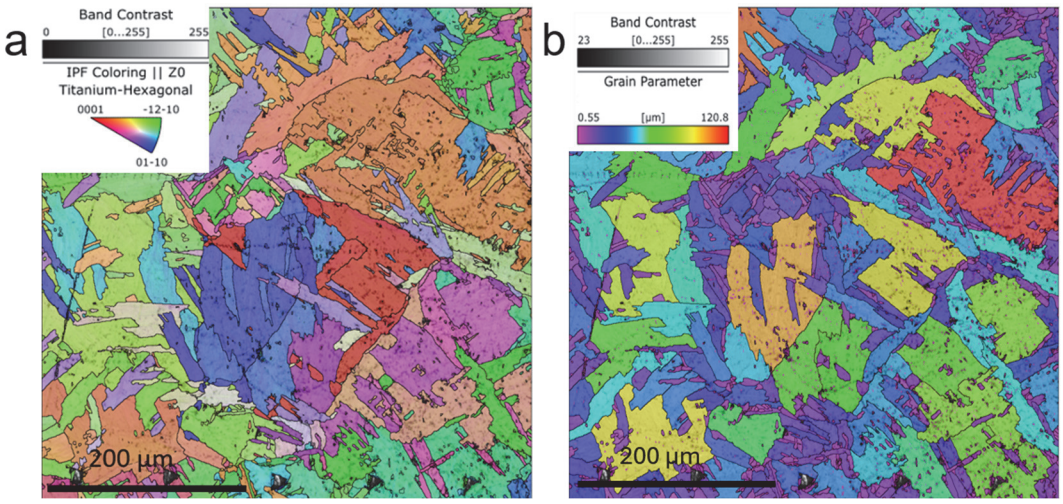

Figure 5: Microstructure of Ti-6Al-4V alloy plate: a) Grain orientation map; b) Grain size map.

Since these methods work in different scales and provide independent measurements it is necessary to explain their limitations. ESPI method allows us to obtain full-field optical evaluations of residual stress and provide the ability to analyze relatively large areas, this technique captures residual stress at macroscopic level (Type I). FEM predictions of residual stress also work in macroscopic level of residual stress. Based on this information we can directly use ESPI data for FEM model validation. However, the FIB-DIC method works at macro-, meso- and microscale level (Type I + Type II + Type III) and we cannot use this method directly. To exclude influence of microscale level (Type 3) we created several rings near the grain boundaries and the resulting values were averaged. This procedure suppresses local fluctuations associated with nanoscale defect structures and dislocation arrangements, which are responsible for Type III stresses. As a result, the processed FIB-DIC data primarily represents the combined contribution of Type I and Type II residual stress. Intergranular residual stresses (Type II) introduce local scatter in the measured values due to grain-to-grain elastic and plastic anisotropy. Previous studies have shown that microscopic stress appears as oscillations around the underlying macroscopic stress distribution [8]. Therefore, the remaining variation in the FIB-DIC measurements can be interpreted as a local "noise" superimposed on the dominant macroscopic trend. Since the magnitude of Type II stresses is typically significantly smaller than the macroscopic stress field, their influence on the overall stress profile is limited. Consequently, the averaged FIB-DIC results reliably reproduce the macroscopic residual stress distribution and can be considered representative of the Type I residual stress component.

As illustrated in Fig. 6, the simulated in-plane residual stress distribution exhibits excellent agreement with both experimental datasets. This consistency confirms that the constitutive model, boundary conditions, and loading protocol in the FEM accurately reproduce the material's mechanical response during unloading, thereby establishing a validated foundation for subsequent analysis of through-thickness stress states after relief. In Fig. 6, the radial coordinate R=0 corresponds to the center of the indentation on the specimen surface, from which the radial distance R is measured.

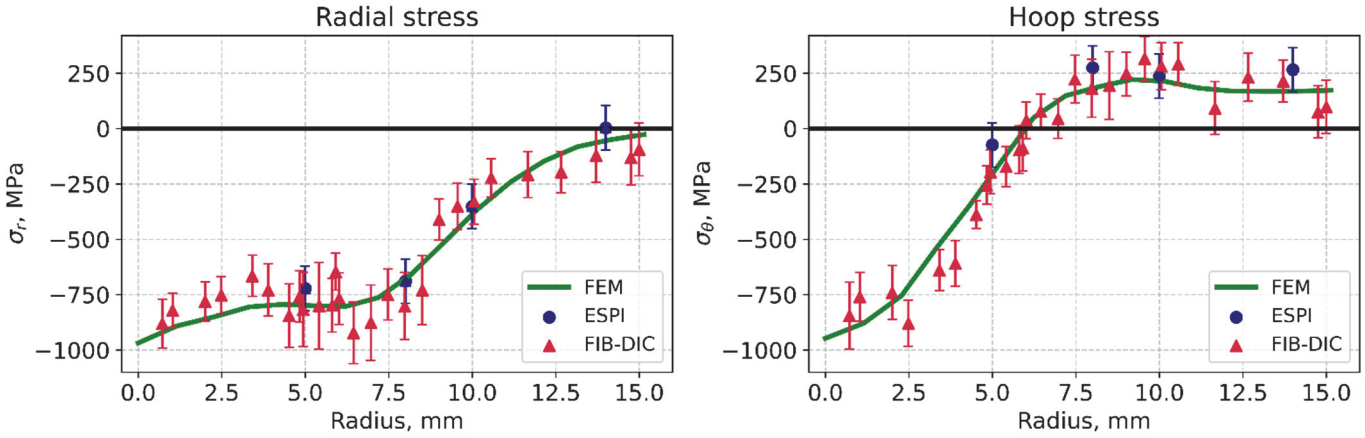

Figure 6: Residual stress in-plane correlation (radial – left; hoop – right).

The second step provides the validation of the FEM model in-depth using the cross-section warp method. The essence of this approach lies in the inherent fundamental mechanics relationship between residual stress and elastic deformation (displacement) that is well known from reciprocal theorems. Reciprocal theorems in mechanics, primarily Betti's reciprocal theorem and Maxwell's theorem [3,18], state that for linear elastic structures, the work done by one system of loads through displacements caused by a second system equals the work done by the second system through displacements caused by the first. This allows inferring stresses from deformations, and vice versa. The well-known manifestation of this concept is the contour method that uses the observed elastic displacements after cutting to deduce (reconstruct) the pre-existing residual stresses in the system prior to cutting [15].

In the contour method the observed deplanation (warp) is used as input for the solution of the second problem through the application of boundary displacement with the opposite sign to an unstressed part. The cross-section warp approach differs in that the observed cutting-induced warp is used as a target for modelling. The model may capture the process that leads to the creation of residual stresses or may be based on eigenstrain representation of the sources of residual stresses [20]. Furthermore, if this kind of direct eigenstrain model or process model can be parameterized, then the cross-section warp method may offer a variational means of model refinement to achieve best agreement with the experiment.

One of the limitations of the method is edge effects caused by the temperature gradient of the wire's electric discharge. The temperature gradient influences the boundaries of the specimen; because of this, the investigation area was limited to 8×20 mm (Fig. 4c). Despite this limitation, we can estimate the most interesting part of the cross-section warp and conclude that the FEM model describes the displacements after relief with high accuracy (Fig. 7).

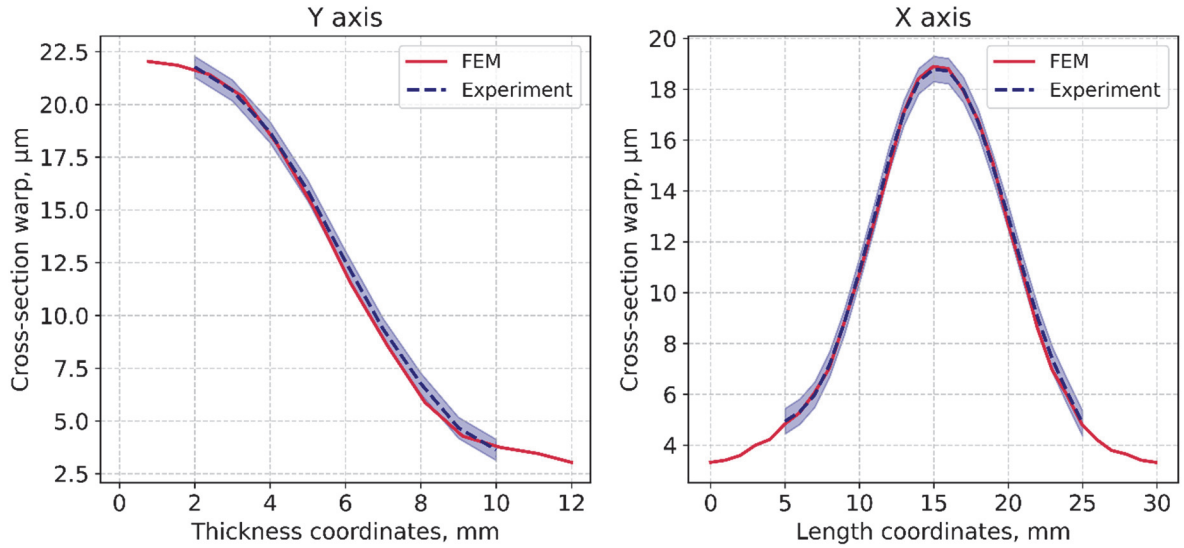

Figure 7: 1D profiles of out-of-plane displacements in the Y axis (left) and X axis (right).

After the validation, either in-plane or in-depth (through thickness) parts of the model, we can determine the quantifiable distribution of residual stress through the entire thickness of the plate. In general, stress distribution follows the scheme shown in Fig. 1. Compressive residual stress induced by one-sided dimpling squeezes tensile stress up to the bottom and boundaries of the specimen. The value of maximum compressive stress is almost three times higher than the maximum value of maximum tensile residual stress (Fig. 8).

For deeper analysis of stress distribution, we evaluate the three representative zones of the specimen: center of dimpled area (R=0 mm), boundary of the specimen (R=30 mm), and the middle area between the center and boundary zones (R=7.5 mm) – as shown in Fig.9 a.

The obtained profiles reveal a characteristic stress redistribution induced by localized plastic deformation during the dimpling process. At the indentation center, both radial and hoop stresses exhibit strong compressive values in the near-surface region, resulting from severe plastic deformation caused by the spherical indenter. With increasing depth, the compressive stresses gradually decrease and eventually transitions to tensile stresses in the lower part of the plate. This transition reflects elastic recovery and the requirement of internal force equilibrium within the material. At the intermediate radius, the magnitude of both compressive and tensile stresses decreases, and the stress gradients become smoother through the thickness. Near the specimen boundary, the residual stresses are significantly smaller and are mainly tensile, indicating that the outer regions of the plate accommodate the global stress balance generated by the localized deformation in the

indentation zone. Overall, the results confirm that one-sided dimpling produces a typical residual stress pattern characterized by compressive stresses near the surface and compensating tensile stresses in the deeper layers of the material.

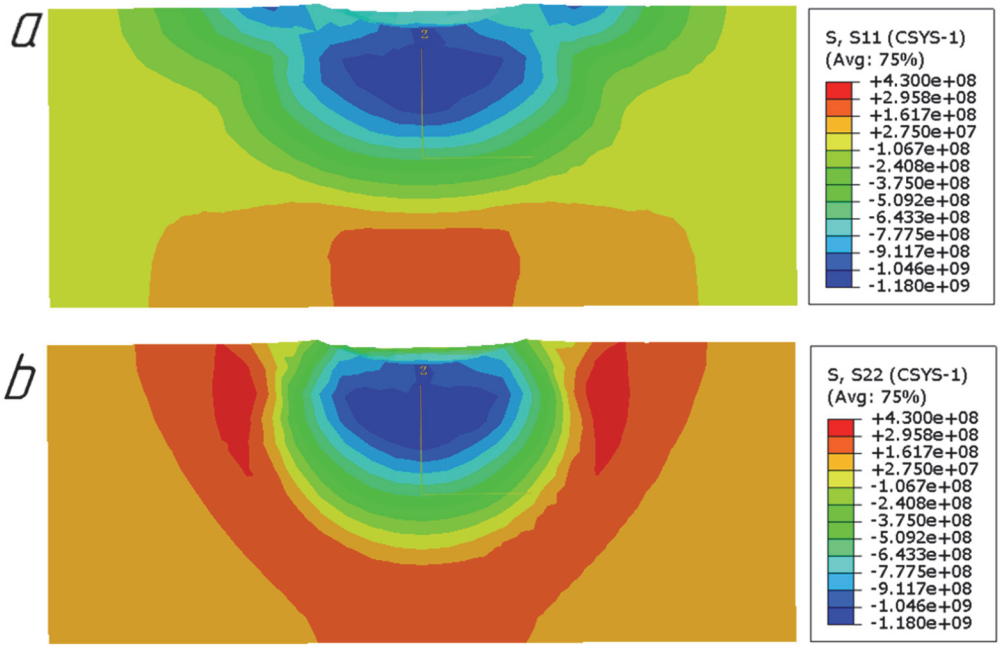

Figure 8: Contour maps of residual stress distribution through thickness after unloading: a) Radial stress presented in Pascals, Pa; b) Hoop stress presented in Pascals, Pa.

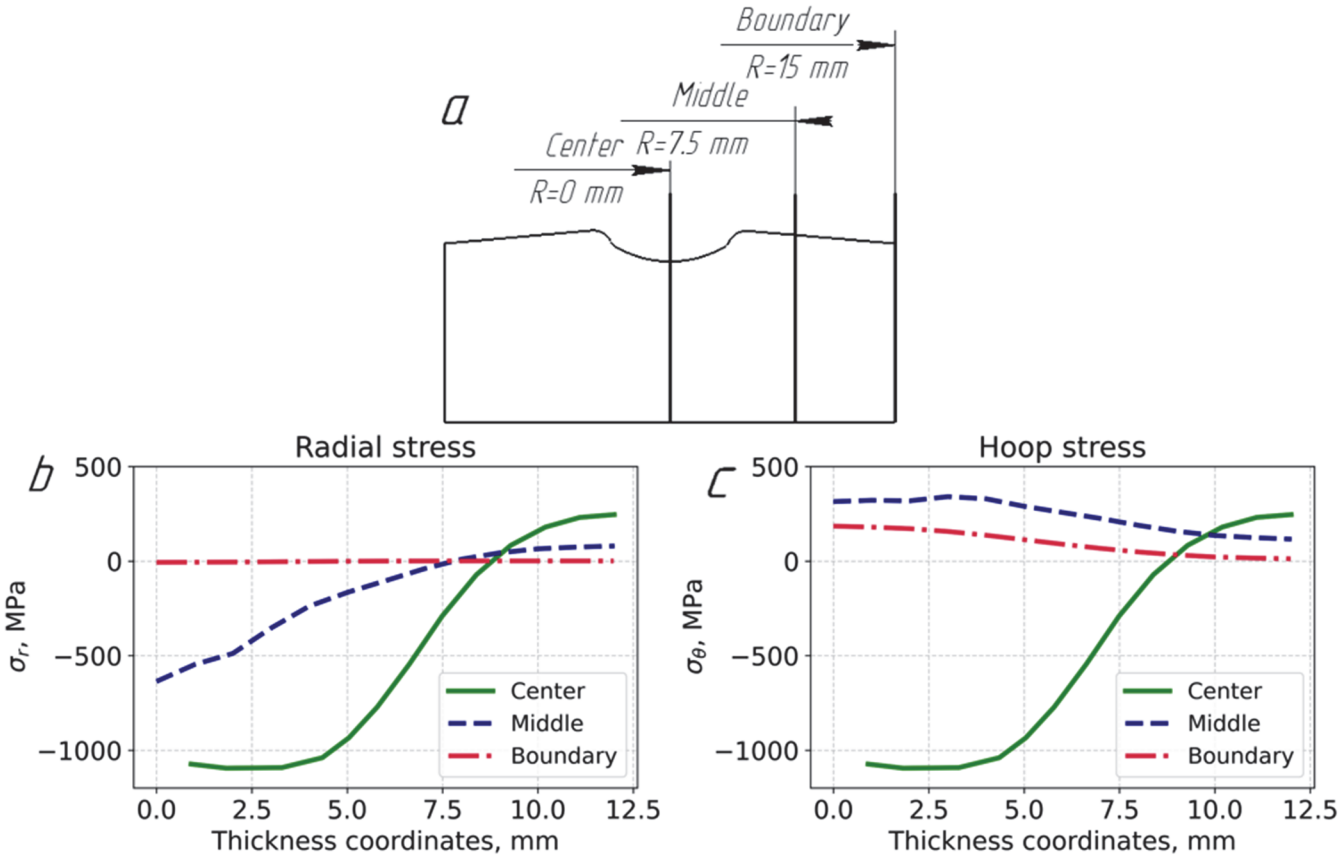

Figure 9: Line profiles of through-thickness residual stress distribution: a) Scheme of residual stress evaluation 1D profiles; b) Radial stress 1D profiles; c) Hoop stress 1D profiles.

The finite element model, validated against both surface measurements and through-thickness displacement data, provides a reliable framework for further parametric analysis of the dimpling process. In future work, the model will be used to systematically investigate how key technological parameters—specifically indentation depth and indenter diameter—affect the magnitude and spatial distribution of compressive residual stresses. These parameters directly control the size of the plastic deformation zone and the degree of elastic constraint in the surrounding material, which in turn determines the resulting residual stress field. By performing a series of controlled numerical simulations with varying indentation depths and indenter diameters, it will be possible to quantify their influence on the peak compressive stresses, the depth of the compressive layer, and the overall uniformity of the stress distribution. Particular attention will be given to identifying parameter combinations that maximize beneficial compressive stresses near the surface while avoiding excessive tensile stresses in the bulk material. The validated model, therefore, serves as an effective predictive tool for optimizing the dimpling process and improving fatigue performance of structural components made from Ti-6Al-4V alloy. Such a parametric study will provide quantitative guidelines for tailoring the residual stress field through appropriate selection of indentation geometry and processing conditions.

Conclusion

This study presents a comprehensive experimental–computational methodology for evaluating residual stresses generated by one-sided dimpling in a Ti-6Al-4V plate. A key advantage of the work is the implementation of a complementary experimental approach combining Electronic Speckle Pattern Interferometry (ESPI) and Focused Ion Beam–Digital Image Correlation (FIB-DIC). These techniques enable reliable determination of in-plane residual stresses at different spatial scales, providing both full-field macroscopic measurements and highly localized micro-scale stress evaluation. The use of two independent experimental methods significantly increases the reliability of the obtained data and provides a solid basis for validation of the numerical model.

Another important contribution of the research is the development of an original technique for residual stress evaluation in the material volume – cross-section warp method. This method combines profilometric measurements of the cross-section of a divided deformed body with finite-element simulation of the stress relief process after cutting. The direct comparison of experimentally measured surface warping with numerical predictions enables validation of the through-thickness residual stress distribution without solving an inverse reconstruction problem.

The fully validated finite element model provides a robust predictive tool for further analysis. In future studies, it will be used to establish how indentation depth and indenter diameter quantitatively influence the magnitude and uniformity of compressive residual stress distribution, enabling optimization of dimpling parameters for improved structural performance.

References

[1] Ahmad, B., Fitzpatrick, M.E. (2016). Minimization and Mitigation of Wire EDM Cutting Errors in the Application of the Contour Method of Residual Stress Measurement, Metall Mater Trans A, 47(1), pp. 301–313. DOI: https://doi.org/10.1007/s11661-015-3231-7.

[2] ASM Handbook Committee ed. (1990). Properties and Selection: Nonferrous Alloys and Special-Purpose Materials, ASM International, DOI: https://doi.org/10.31399/asm.hb.v02.9781627081627.

[3] Auli, J.S., Bayad, A., Beck, M. (2017). Reciprocity theorems for Bettin–Conrey sums, Acta Arith., 181(4), pp. 297–319. DOI: https://doi.org/10.4064/aa8580-8-2017.

[4] Bjørheim, F., Siriwardane, S.C., Pavlou, D. (2022). A review of fatigue damage detection and measurement techniques, International Journal of Fatigue, 154, p. 106556. DOI: https://doi.org/10.1016/j.ijfatigue.2021.106556.

[5] Chang, S., Zhang, K., Tan, J., Tu, S. (2024). The effect of residual stress on high-cycle fatigue properties and its evaluation method of Ti-6Al-4V alloy, Fatigue Fract Eng Mat Struct, 47(10), pp. 3633–3645. DOI: https://doi.org/10.1111/ffe.14397.

[6] Dölle, H. (1979). The influence of multiaxial stress states, stress gradients and elastic anisotropy on the evaluation of (Residual) stresses by X-rays, J Appl Crystallogr, 12(6), pp. 489–501. DOI: https://doi.org/10.1107/S0021889879013169.

[7] Eleonsky, S., Pisarev, V., Statnik, E., Salimon, A., Korsunsky, A. (2024). Residual stress determination by blind hole drilling and local displacement mapping in aluminium alloy aerospace components, Frattura Ed Integrità Strutturale, 18(69), pp. 192–209. DOI: https://doi.org/10.3221/IGF-ESIS.69.14.

[8] Everaerts, J., Salvati, E., Uzun, F., Romano Brandt, L., Zhang, H., Korsunsky, A.M. (2018). Separating macro- (Type I) and micro- (Type II+III) residual stresses by ring-core FIB-DIC milling and eigenstrain modelling of a plastically bent titanium alloy bar, Acta Materialia, 156, pp. 43–51. DOI: https://doi.org/10.1016/j.actamat.2018.06.035.
[9] Kim, J., Lee, K., Kwon, D., Schajer, G.S. (2025). Evaluation of Non-equi-biaxial Residual Stresses from the Surface Displacements Around a Single Indentation, Met. Mater. Int., 31(10), pp. 2919–2930. DOI: https://doi.org/10.1007/s12540-025-01923-w.
[10] Korsunsky, A.M., Sebastiani, M., Bemporad, E. (2009). Focused ion beam ring drilling for residual stress evaluation, Materials Letters, 63(22), pp. 1961–1963. DOI: 10.1016/j.matlet.2009.06.020.
[11] Molent, L., Dixon, B. (2020). Airframe metal fatigue revisited, International Journal of Fatigue, 131, p. 105323. DOI: https://doi.org/10.1016/j.ijfatigue.2019.105323.
[12] Naveed, N. (2018). Experimental study of the effects of wire EDM on the characteristics of ferritic steel, at a micro-scale on the contour cut surface, Metall. Res. Technol., 115(4), p. 413. DOI: https://doi.org/10.1051/metal/2018032.
[13] Pisarev, V., Odintsev, I., Eleonsky, S., Apalkov, A. (2018). Residual stress determination by optical interferometric measurements of hole diameter increments, Optics and Lasers in Engineering, 110, pp. 437–456. DOI: https://doi.org/10.1016/j.optlaseng.2018.06.022.
[14] Prime, M.B. (2018). The Two-Way Relationship Between Residual Stress and Fatigue/Fracture., In: Carroll, J., Xia, S., Beese, A.M., Berke, R.B., Pataky, G.J. eds., Fracture, Fatigue, Failure and Damage Evolution, 7, Cham, Springer International Publishing, pp. 19–23.
[15] Prime, M.B., DeWald, A.T. (2013). The Contour Method., In: Schajer, G.S. ed., Practical Residual Stress Measurement Methods, 1st ed., Wiley, pp. 109–138.
[16] Souiyah, M., Muchtar, A., Ariffin, A.K. (2011). Finite Element Analysis of Indentation Cracks for Brittle Materials under Static Loading, KEM, 462–463, pp. 160–165. DOI: https://doi.org/10.4028/www.scientific.net/KEM.462-463.160.
[17] Sunder, R. (2016). Why and How Residual Stress Affects Metal Fatigue., In: Parinov, I.A., Chang, S.-H., Topolov, V.Yu. eds., Advanced Materials, vol. vol. 175, Cham, Springer International Publishing, pp. 489–504.
[18] Tarnai, T., Lengyel, A. (2007). Reciprocal Theorems: An Old Subject Revisited, International Journal of Mechanical Engineering Education, 35(2), pp. 138–147. DOI: https://doi.org/10.7227/IJMEE.35.2.4.
[19] Tavares, S.M.O., De Castro, P.M.S.T. (2017). An overview of fatigue in aircraft structures, Fatigue Fract Eng Mat Struct, 40(10), pp. 1510–1529. DOI: https://doi.org/10.1111/ffe.12631.
[20] Uzun, F., Korsunsky, A.M. (2025). Reconstruction of residual stresses in additively manufactured Inconel 718 bridge structures using contour method, Int J Adv Manuf Technol, 137(9–10), pp. 4573–4582. DOI: https://doi.org/10.1007/s00170-025-15417-x.
[21] Vaara, J., Kunnari, A., Frondelius, T. (2020). Literature review of fatigue assessment methods in residual stressed state, Engineering Failure Analysis, 110, p. 104379. DOI: https://doi.org/10.1016/j.engfailanal.2020.104379.
[22] Webster, G.A. (2000). Role of Residual Stress in Engineering Applications, MSF, 347–349, pp. 1–11. DOI: https://doi.org/10.4028/www.scientific.net/MSF.347-349.1.

Declaration of competing interest

The authors declare no competing interests.

Acknowledgment

This study was carried out under the Agreement for the provision of grant funding from the federal budget for large scientific projects in priority areas of scientific and technological development of the Russian Ministry of Science and Higher Education, no. 075-15-2024-552.